Assessing the impact of Zn-MgO-xC_n Ternary Coatings on A36 Low Carbon Steels for Oil and Gas Pipeline Applications

B. U. Anyanwu[1*], O. O. Oluwole[2], O. S. I. Fayomi[3, 5*], A. O. Olorunnisola[4], A. P. I. Popoola[5], S. I. Kuye[1], W. B. Wan Nik[6] and K. M. Oluwasegun[7]

[1]*Department of Mechanical Engineering, Federal University of Agriculture, Abeokuta, Nigeria*
[2]*Department of Mechanical Engineering, University of Ibadan, Nigeria*
[3]*Department of Mechanical and Biomedical Engineering, Bells University of Technology, Ota, Nigeria*
[4]*Department of Wood Products Engineering, University of Ibadan, Nigeria*
[5]*Department of Chemical, Metallurgical and Materials Engineering, Tshwane University of Technology, Pretoria, South Africa*
[6]*Faculty of Ocean Engineering Technology and Informatics, University of Malaysia Terengganu, Malaysia*
[7]*Department of Mechanical and Manufacturing Engineering, University of Manitoba, Winnipeg, Manitoba, Canada*
*Corresponding authors: anyanwubu@funaab.edu.ng, osfayomi@bellsuniversity.edu.ng

Received 19/12/2021; accepted 10/04/2022
https://doi.org/10.4152/pea.2023410404

Abstract
Issues regarding corrosion have become a substantial source of expenditure for oil and gas industries. Apart from that, oil spillages resulting from leakages in pipelines pose severe environmental challenges, such as pollution and fire outbreaks. A36 LCS is commonly used for fabricating oil and gas pipelines, due to its availability and cost. The aim of this study was to deposit Zn-MgO-xC_n CC on A36 LCS substrates, to improve their CRS in acidic media, through the ED route. ΔW corrosion determination technique was used for determining the developed coatings CR. The CC surface morphology and phase evolution were determined by OPM, SME and X-RD. The results showed that all the developed CC offered lower CR values than that of the A36 LCS substrate, which was 5.4392 mm/y. Sample D4 (20 g Zn and 20 g MgO-C_n) had the lowest CR value of 0.7199 mm/y, corresponding to a coating E of 86% on the substrate. Finally, among the developed coatings, sample E1 (Zn and 20 g MgO) gave the highest CR values of 2.1030 mm/y, with an E value of 61%. The study showed that the CC were able to form protective barriers on the substrate in the corrosive media.

***Keywords**:* CC, NP, substrates and corrosion.

Introduction•

A36 LCS has a low carbon content in the range from 0.25 to 0.29. It is employed in several engineering applications, because of its good mechanical strength, great

• The abbreviations and symbols definitions lists are in page 311.

availability and low cost [1-5]. It has been reported that the majority of the oil pipeline networks for petroleum products transportation in Nigeria are made of LCS [6-7]. However, due to the chemical nature of the fluids transported by these pipelines, and to the environment that surrounds their installation, the chances of corrosion are high. A36 LCS has been reported to severely corrode in highly acidic, salty, and alkaline environments, making it a subject of interest for most material experts [7-10]. Related to the issues of substantial sources of expenditure for the oil and gas industries, especially in Nigeria, which is the leading oil producer in Africa, there are reports that they are being affected by consistent supply disruptions, due to oil spillages [8]. Although many of the spillages are due to pipeline vandalism, their majority results from corrosion in most of the pipelines sections [6-7]. The effects of these spillages, such as environmental pollution, loss of human lives and properties damage, cannot be overemphasized [6-8]. This is why experts are in continuous search for technological advancements in this area, which will reduce the corrosion trend of A36 LCS, among other materials.

Several methods have been developed and reported for LCS corrosion control and prevention in different media. Among these methods, metal surface modifications, in the form of CC, have been reported as effective [9-10].

CC applications are one of the surface modifications in practice, and, in recent times, they have been effectively used for enhancing LCS external and structural integrity [9-11]. However, a CC must stick to the substrate, so that it may reach maximum E%. The coating must also have good throw power and edge coverage [10, 12]. There are different methods employed in surface coating technology. Laser, plasma, electroless and SG coatings, hot dipping and electrolytic deposition, etc., have been reported as successful surface modification methods [9]. However, studies have also shown that coating by the ED route is cost-effective, easy to use, and offers high deposition rate [12-13]. The coating produced by the ED process is more homogenous, and has less defects than those produced by other processes. ED is an Ec process employed for materials surface modifications. During ED, the coating(s) layer(s) are deposited on a substrate, through Ec reactions occurring at the electrode/electrolyte interface [14]. Such layers are deposited on the substrate material, in order to improve its CRS, electrical, magnetic, mechanical, thermal and aesthetic properties. The ED process can be performed using DC or PC. In the DC method, electrical current is continuously applied, while, in the PC technique, it is swiftly alternated between two different current values. Parameters, such as bath temperature, agitation, contents, concentration, pH, I and deposition time, play vital roles in ensuring good coating deposits on the substrates [13-14].

Furthermore, various organic and inorganic materials have been deposited on LCS surfaces. Zn is highly demanded for this purpose, due its useful sacrificial features, and formation of protective barriers between the substrate and the corrosive environment. Nevertheless, Zn still decomposes in service, especially with high temperatures and in acidic media [10-11]. This is why Zn coatings have been further modified with other organic materials, such as ceramics, metallic oxides and polymers, etc. These materials are dispersed in aqueous solutions of Zn salts, and used at their nanoscales, in order to obtain excellent coatings with incredible mechanical and CRS properties. Zn-ZnO-SiO_2 nano CC development on a MS substrate by ED means was reported by Rezaee N. et al. [15]. Using

PDP technique, they have studied the coatings corrosion behaviour in a 3.65% NaCl medium. The developed coatings improved MS CRS properties over those of the uncoated substrate. In a separate study by Odetola P. et al., TiO_2 NP were co-deposited with Zn on a sulphate bath (pH 4.5), using the ED technique [11]. The coatings corrosion behavior was assessed by Ec polarization, impedance and ΔL methods. TiO_2 incorporation in the coating led to an improvement in the CC CRS property, as compared to the pure Zn coatings. In their study, Lei T. et al. have developed nano crystalline $Zn_3(PO_4)_2$ coatings on a MS surface, using ZnO NP. PDP and Ec impedance studies were carried out in a 3.5% NaCl solution. The results showed that the developed CC yielded a greater θ, and had higher CRS than that of the MS substrate [16]. Also, in a research by Jinxia M. et al., low temperature $Zn_3(PO_4)_2$ conversion coatings were formed on a MS substrate [17]. In that study, PDP was used to evaluate the phosphated samples corrosion behaviour in a 3.5 wt% NaCl solution. The results showed that the phosphate coating CRS was significantly enhanced.

In a study reported by [18], an MgO coating was deposited, by anodic ED, on an Mg alloy, for its corrosion protection, in a 6 M KOH solution. PDP measurements showed that MgO protective coatings improved Mg alloy CRS properties, compared to the bare metallic Mg.

Zn coatings with a blend of biopolymers and metallic oxide NP deposited on MS substrates have never been reported in any study. Presently, there are few studies on bio-C ED, despite its potential [19], which forms the basis of the present research.

The most abundant and readily available biopolymer, currently in use for material properties modification, is C [20-26]. It has been widely used in areas, such as electrically conductive coatings, heavy metals removal and adsorbent materials, because of its renewable, mechanical and CRS properties, and environmentally friendly characteristics [20-23]. C_n particles have been successfully co-deposited, in separate, on Ni, Cu, Ag and In_2O_3 [20-25].

The aim of this study was to deposit Zn-MgO-xC_n fibres on A36 LCS substrates in acidic media, for their improved structural and CRS properties, through DC ED route. ΔL technique was used to determine the deposited coatings CR values. The CC surface morphologies and phase evolution were determined by SME and X-RD, respectively. C_n fibres were extracted from *Hibiscus cannabinus*, and mixed in different proportions with MgO NP. MgO has excellent thermal and CRS properties [27-28]. Also, C_n fibres possess incredible mechanical and CRS properties [20-26]. The combined qualities of these NP were expected to improve the substrate (which is commonly applied in pipeline installations in the Nigerian oil and gas industries) CRS properties.

Experimental methods

The experimental techniques adopted in this study are in line with procedures outlined in highly rated journals and standard codes. The employed materials and chemicals included: a 30 x 20 x 4 mm Zn bar (MW = 65.38; purity = 99.9%; mp = 420 ºC; and bp = 907 ºC); 200 g MgO nanoparticles (MgO = 99.5%, CaO = 0.3%, Cl = 0.02%, Na = 0.02% and SO_4 = 0.16%; particle size = 20 to 80 nm; mp = 2800 ºC; bp = 3600 ºC); analytical grade $ZnCl_2$ (MW = 136.29 and purity = 98%); glycine; and thiourea. All chemicals were sourced from a chemical vendor in Ibadan, Nigeria. Also, about 150 g N_c fibers

(crystallinity index = 74%; size = 10 to 50 nm; and C content = 95%) were sourced from the Agricultural Research Institute in Nigeria. 20 g each of MgO NP were mixed with different proportions (from 5 g to 20 g) of C_n fibres, with 10% acidic ionic liquid, using a homogenizer [15-16]. This mixture formed the NP blend that was employed in the study. The substrate, A36 LCS (0.24 to 0.30% carbon) was purchased from a steel distributor in Agbara, Lagos State, Nigeria.

Bath contents and deposition

A36 LCS samples, with the chemical composition shown in Fig. 1, were polished with emery papers up to 600 grits, in order to erase any existing impurities in them, and to provide mirror-like scale free defects. They were then cut into sections of 50 x 20 x 2 mm, degreased in trichloroethylene, rinsed in water, and activated by immersing them in a 10% HCl solution, for 10 s. The bath contents were made of analytical grade chemicals and distilled water: ZnCl, glycine, thiourea, MgO NP and C_n fibres (100, 10, 10, 20 and 5 to 20 g/L, respectively).

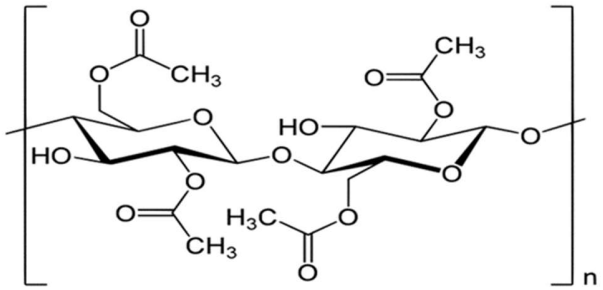

Figure 1. C_n molecular structure.

NP composition and applied voltage are shown in Table 1.

Table 1. NP composition.

Experiment no.	NP blend	Voltage (V)	Sample ID
1	20 g MgO-5 g C_n	0.3	D1
2	20 g MgO-10 g C_n	0.3	D2
3	20 g MgO-15 g C_n	0.3	D3
4	20 g MgO-20 g C_n	0.3	D4
Control 2	20 g MgO	0.3	E1
Control 1	a-r substrate	-	A

The pretreated substrate and the 99.9% Zn bar were prepared as cathode and anode, respectively. The immersion depth and distance between the anode and cathode were kept constant. The bath solution was heated and maintained at 40 ºC, in order to admix and allow for the particles dissolution. It was then continuously stirred with a mechanical stirrer, up to 1000 rpm, so as to achieve electrolytes uniformity. The deposition was carried out with NP varying concentrations, of 5.5 pH, at a set potential of 0.3 V and a constant I of 2.0 A/cm^2, for 20 min. After deposition,

the samples were rinsed in distilled water, for 5 s, and then dried at air. The most distinguished step in this study was to admix Zn with various quantities of 20 MgO-xC_n particulates, to form thin CC on the substrates. The NP coordination with metal ions was produced by the anodic Ec oxidation, which enabled them to be deposited on the electrode. The deposition mechanism was attained by the incorporation of 20 MgO-xC_n composites weight fractions in the Zn^{2+} basic electrolyte [9-11].

CR analysis of the developed CC and substrate

The corrosion behavior of the developed CC and substrate was studied by the ΔL technique. This was done at room temperature, in a 1 M HCl medium. The adopted procedures were in line with ASTM G1-03 (standard practice for preparing, cleaning and evaluating corrosion test specimens) and ASTM G31-72 (standard practice for laboratory immersion corrosion testing of metals). Coupons measuring 1 x 1 cm were weighed with a high precision Mettler Toledo analytical balance, before and after immersion in the corrosion medium, for 720, 1440, 2160 and 2880 h. The coupons were then removed, rinsed with water and acetone, and dried. The difference in weight was taken and recorded. Equation 1 was then used to calculate the samples CR (mm/year).

$$CR = \frac{8.76 \times 10^4 \, \Delta W}{\rho A T} \quad . \tag{1}$$

where ρ = sample density (g/mm^3), A = exposed area (cm^2) and T = exposure time (h).

$$E\ (\%) = (1 - \frac{CR_C}{CR}) \times 100 \quad . \tag{2}$$

$$\theta = (1 - \frac{CR_C}{CR}). \tag{3}$$

According to [5-7, 29], equations 2 and 3 were used to compute E% values and the developed coatings θ. CR_c and CR are the corrosion rates with and without the coatings (i.e. the substrate), respectively.

Samples characterization

The developed coatings and substrate microstructures were obtained via an OPM, with a 10X magnification. This was done after the corrosion analysis. Also, a TESCAN SME, at a magnification of 1000X, was used to determine the developed coatings and substrate surface and internal morphologies, in terms of grains refinement and uniformity. The samples phase evolution and crystallographic parameters were measured with an X-RD, and their phase presence and quantification were determined by matching them via an X'PERT high-score software equipped with a PDF4/ICDD database (Table 1).

Results and discussion

Characterization of the developed CC

Fig. 2 shows the SEM/EDS spectra of the a-r A36 LCS substrate. It is seen that carbon content (0.26%) falls within the acceptable values for steel. The spectra were also devoid of any coating deposits, as they were expected to appear, after the actual ED.

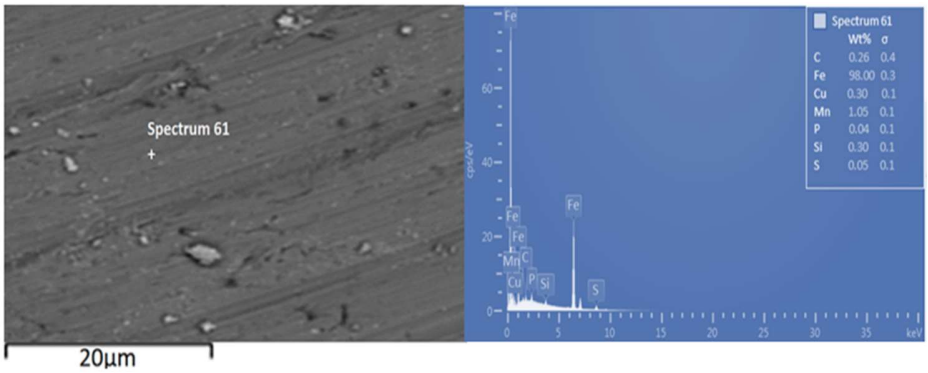

Figure 2. SEM/EDS spectra of the a-r A36 LCS.

Fig. 3 shows the SEM/EDS spectra of the developed Zn-MgO-xC_n particles coatings. The spectra were taken prior to the corrosion study. All the coatings had good adherence, proper uniformity, and were free from porosity. The coatings also displayed good edge protection and throw power, which promoted and enhanced their structural integrity and performance [10, 29]. However, samples D4 showed better coatings attributes. This may be attributed to the NP blends increased concentration in the bath, as they were more dispersed and deposited on the substrate [12-13].

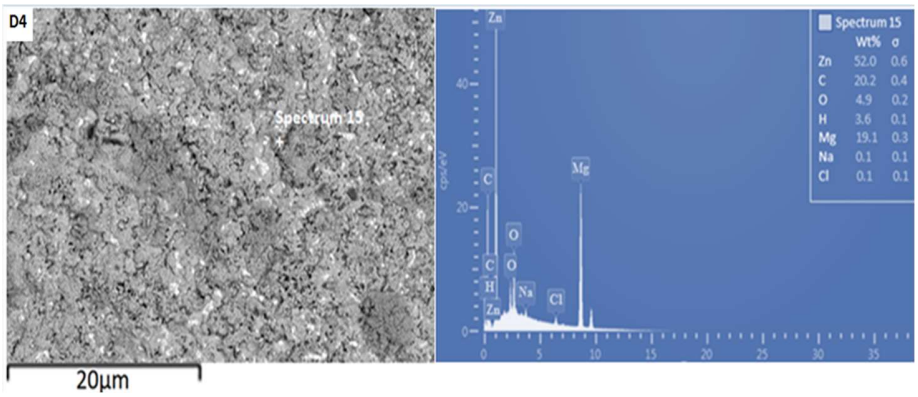

Figure 3. SEM/EDS spectra of the developed Zn-MgO-xC_n CC.

Fig. 4 denotes the SEM/EDS spectra of the control sample 2, coated with the Zn-MGO blend only.

The structure reveals a good coating adherence, edge protection and throw power, but with less fine grains, compared with the Zn-MgO-xC_n coatings.

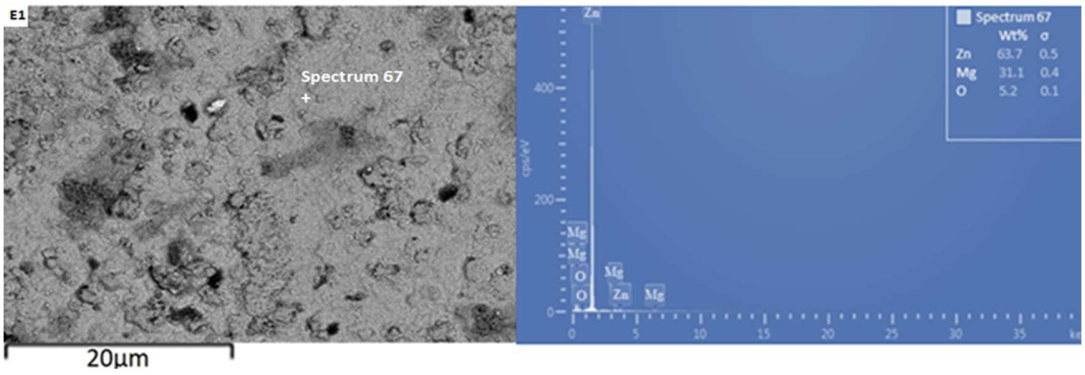

Figure 4. SEM / EDS spectra of the developed Zn-MgO CC.

Again, XRD spectra of Zn-MgO-xC_n coatings, as shown in Fig. 5, presented evidence of phase evolutions, indicating crystallized Zn, C II and periclase (which is a form of MgO) peaks. The crystallized C II occurred at the 20° diffraction peak and 002 crystallographic plane.

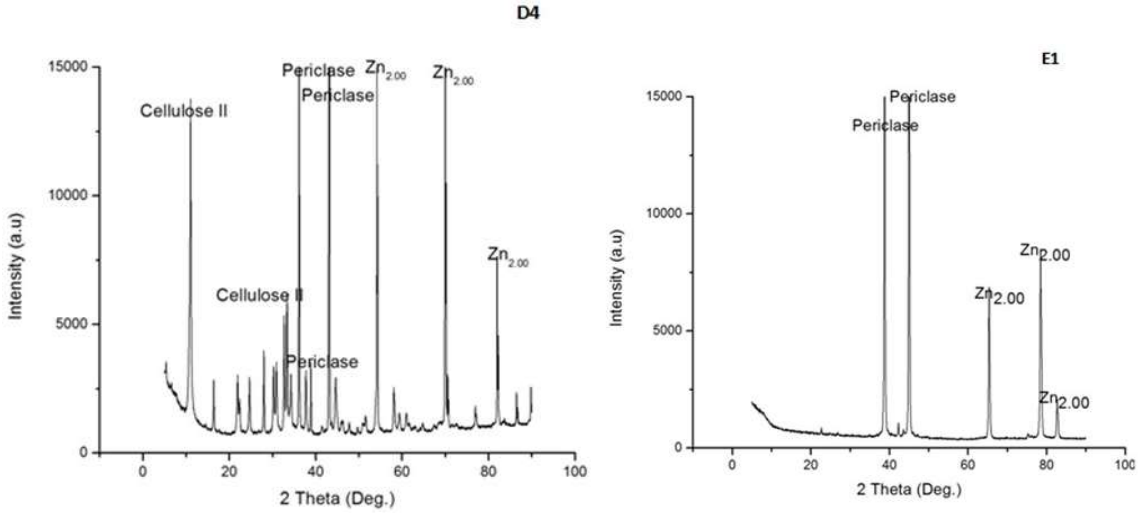

Figure 5. XRD spectra of the developed CC.

Studies have shown that the crystallized forms of C appear as alpha or beta (C I and C II) [24].

Periclase is also seen as one of the phases evolved in the XRD spectra, occurring mainly at the 43° diffraction peak, with 200 crystallographic planes. Zn had the most active phase, with more peaks than the others, and this is due to the fact that its based anode was employed in the study. The phase presence in the coatings was further affirmed by EDS spectra. All coatings developed from the Zn-MgO-xC_n particles had Zn, Mg, C and a small percentage of O and H in their compositions. C, O and H contents may have come from the C_n particles used [28]. Samples E1 (control samples 2), only coated with

MgO nanoparticles, were mainly composed of Zn and Mg. XRD spectra (Fig. 5) also confirmed the phase presence in the samples. It can be seen that MgO (periclase) and Zn were the most evolved phases in the coatings.

CC corrosion study

Corrosion data results for the substrate and developed coatings are presented in Tables 2 and 3.

Table 2. Corrosion data of the substrate and developed coatings.

Time	720 h		1440 h		2160 h		2880 h		Aver.
Sample ID	ΔW (g)	CR (mm/y)	ΔW (g)	CR (mm/y)	ΔW (g)	CR (mm/y)	ΔW (g)	CR (mm/y)	CR (mm/y)
D1	0.1192	1.8437	0.2280	1.7701	0.3201	1.6535	0.4141	1.6034	1.7177
D2	0.0921	1.4213	0.1700	1.3214	0.2521	1.2994	0.3261	1.2645	1.3267
D3	0.0551	0.8515	0.1061	0.8241	0.1550	0.7981	0.1891	0.7341	0.8020
D4	0.0511	0.7860	0.0941	0.7310	0.1350	0.6984	0.1712	0.6641	0.7199
E1	0.1400	2.1752	0.2750	2.1288	0.3981	2.0591	0.5291	2.0490	2.1030
A	0.4330	6.7124	0.8650	6.7022	0.8660	4.4740	0.9983	3.8681	5.4392

Table 3. Coatings E% and θ.

Samples	θ	E%
D1	0.68	68
D2	0.76	76
D3	0.85	85
D4	0.86	86
E1	0.61	61

It can be seen that CR values decreased for all samples, as the coupons exposure time in the corrosive media increased. CR values also decreased with the increase in the NP blends concentration in the coating bath. The CR values are functions of the corresponding ΔW, which was higher for all samples as the exposure time was increased (Fig. 6).

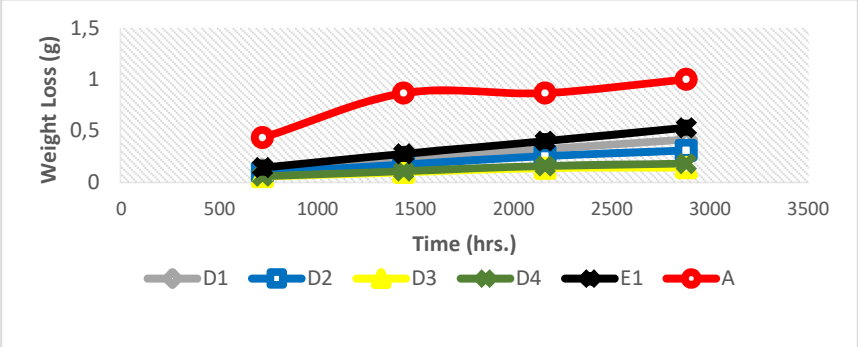

Figure 6. ΔW rate for all samples after exposure in the corrosive media.

The a-r samples ΔW started decreasing after 1440 h of exposure, but later increased after 2160 h of exposure. This may not be unconnected with the substrate passivation tendencies [1-7]. All the developed CC, as seen from the tables, offered lower CR values than those of the a-r samples. This is due to the fact that the coatings reduced the ions penetration from the corrosive media into the LCS sites active positions. Again, the results showed that sample D4 (20 g Zn and 20 g MgO-C_n) had the lowest average CR value of 0.7199 mm/y, while the a-r samples had an average CR value of 5.4392 mm/y. The coatings offered θ of 0.86 and E of 86% to the substrate. Among the developed coatings, the highest CR value of 2.1030 mm/y, with θ of 0.61 and E of 61%, was obtained by sample E1 (20 g Zn and MgO), which served as one of the control samples (see Table 3). The corrosion mechanism in this study was generally accompanied by HER, resulting in the substrate dissolution [29]. The samples anodic dissolution in the media depended on the cathodic reactions shown in equation (4).

$$2H^{+}_{(aq)} + 2e^{-} \Leftrightarrow H_{2(g)} \quad \text{.....(4)}$$

Hence, the anodic reaction involved the samples dissolution, in order to balance the charge, as shown in equation (5), with the overall reactions in equation (6).

$$Fe_{(s)} \Leftrightarrow Fe^{2+}_{(aq)} + 2e^{-} \quad \text{.....(5)}$$

$$Fe + 2H^{+} \Leftrightarrow Fe^{2+} + H_2 \quad \text{.....(6)}$$

Once the samples came in contact with the corrosive media, the ions migrated from the metal surface to the bulk of the solution, which resulted in corrosion. However, this migration was blocked by the protective Zn-MgO-xC_n and Zn-MgO coatings on the substrates, thereby hindering a further reaction between the samples and the corrosive media. This effect significantly lowered the substrates samples CR. The coatings E% may be traceable to chemical affinities of its reactive atoms, such as Zn, Mg, O and C, with the LCS surface, thus preventing the attack by Cl^{-} [20, 29].

Fig. 7 shows the substrate (A) and the developed CC OPM images. They were taken after the samples were exposed to the corrosive media.

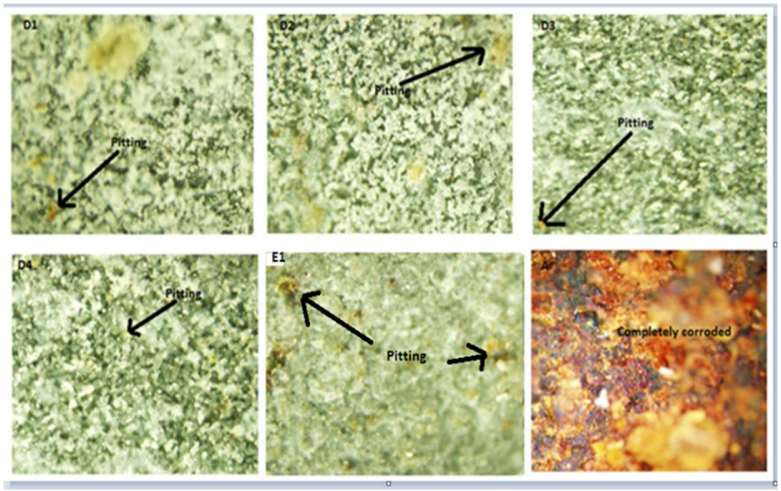

Figure 7. OPM images of all samples after exposure in the corrosive media.

It can be seen in the images that the a-r sample suffered massive corrosion caused by the attack from the corrosive media. The corrosive products formed on the LCS surface were more numerous than those seen on the developed coatings surfaces. In fact, few pitting corrosion spots were seen on the developed coatings surfaces, especially on sample D4 (20 g Zn and 20 g MgO-C_n). This may be connected with the fact that the sample showed better coating adherence, throw power and edge coverage, as revealed from SEM spectra. Studies have shown that coatings with adequate throw power, adherence and edge coverage offer wonderful performances during service [12].

Conclusion

Zn-MgO-C_n CC were successfully deposited on the A36 LCS substrates by ED route. The coatings showed good uniformity, coating adherence, edge coverage and throw power. This is the reason why they had lower CR values than those from the substrate employed in the study. Sample D4 (20 g Zn and 20 g MgO-C_n) had the lowest CR value of 0.7199 mm/y, corresponding to an E of 86% on the substrate. The study has shown that the coatings were able to block ions migration from the substrate to the corrosive media, thereby hindering a further reaction that would have resulted in uncontrolled metal dissolution. This effect significantly lowered CR values and improved CRS properties of the substrate commonly applied for pipeline installations in the Nigerian oil and gas industries.

Acknowledgements

The researchers acknowledge the support of the following bodies in starting and executing the study: Management of Federal University of Agriculture, Abeokuta, Ogun State, Nigeria; Tertiary Education Trust Fund (TetFund), Nigeria; Management of Covenant University, Ota, Ogun State, Nigeria; Post-graduate College, University of Ibadan, Nigeria; and Management of Tshwane University of Technology, Pretoria, South Africa.

Conflict of interest

The researchers declare that there was no conflict of interest during and after the study.

Authors' contributions

B. U. Anyanwu: conceived and wrote the paper. **O. O. Oluwole**: conceived and designed the analysis. **O. S. I. Fayomi**: collected the data; wrote the paper. **A. O. Olorunnisola**: designed the analysis; supervised the work. **A. P. I. Popoola**: performed the analysis. **S. I. Kuye**: inserted data or analysis tools. **W. B. Wan Nik**: Incorporated new ideas; interpreted data. **K. M. Oluwasegun**: interpreted the analyses.

Abbreviations

a-r: as-received
bp: boiling point
C: cellulose
CaO: calcium oxide
CC: composite coatings
C_n: nanocellulose
CR: corrosion rate
CRS: corrosion resistance
DC: direct current
E%: protection efficiency
Ec: electrochemical
ED: electrodeposition
EDS: energy dispersive spectroscopy
HCl: hydrochloric acid
HER: hydrogen evolution reaction
I: current density
In_2O_3: indium oxide
KOH: potassium hydroxide
LCS: low carbon steel
MgO: magnesium oxide
mp: melting point
MS: mild steel
MW: molecular weight
NaCl: sodium chloride
NP: nanoparticles
OPM: optical microscopy
PC: pulse current
PDP: potentiodynamic polarization
SEM: scanning electron microscopy
SG: sol-gel
SiO_2: silicon dioxide
SO_4: sulphate ion
TiO_2: titanium dioxide
X-RD: x-ray diffractometry
Zn-MgO-xC_n: zinc-magnesium oxide-nano cellulose
$Zn_3(PO_4)_2$: zinc phosphate
ZnO: zinc oxide

Symbols definition

ΔW: weight loss
θ: surface coverage

References

1. Tang Y, Yang X, Yang W et al. A preliminary investigation of corrosion inhibition of mild steel in 0.5 M H2SO4 by 2-amino-5-(n-pyridyl)-1,3,4-thiadiazole: polarization, EIS and molecular dynamics simulations. Corros Sci. 2010;52(5):1801-1808. https://doi.org/10.1016/j.corsci.2010.01.028

2. Herrag L, Hammouti B, Elkadiri S. Adsorption properties and inhibition of mild steel corrosion in hydrochloric solution by some newly synthesized diamine derivatives: Experimental and theoretical investigations. Corros Sci. 2010;52(9):3042-3051. https://doi.org/10.1016/j.corsci.2010.05.024
3. Abiola OK, Oforka NC. Inhibition of Corrosion of Mild Steel in Hydrochloric Acid. J Corros Sci. Eng. 2002;3:21-26.
4. Noor EA, Al-Moubaraki AH. Corrosion Behavior of Mild Steel in Hydrochloric Acid Solutions. Int J Electrochem Sci. 2008;3:806-818.
5. Fayomi OSI, Popoola API. Development of smart oxidation and corrosion resistance of multi-doped complex hybrid coatings on mild steel. J Alloys Compd. 2015;637:382-392. https://doi.org/10.1016/j.jallcom.2015.02.154
6. Unueroh U, Omonria G, Efosa O et al. Pipeline Corrosion control in Oil and Gas Industry: A case study of NNPC /PPMC System 2A Pipeline. Nig J Technol (NIJOTECH). 2016;35(2):317-320. https://doi.org/10.4314/njt.v35i2.11
7. Popoola API, Fayomi OSI. Performance evaluation of zinc deposited mild steel in chloride medium. Int J Electrochem Sci. 2012;6:3254-3326.
8. Fayomi OSI, Joseph OO, Popoola API. Structural properties and micro-hardness performance of induced composite coatings filled with *Cocosnucifera*-tin functionalized oxide. Ener Proceedia. 2017;119:910-915. https://doi.org/10.1016/j.egypro.2017.07.144
9. Praveeen BM, Venkatesha TV. Electro-deposition and corrosion resistance properties of Zn-Ni/Tio2 nano composite coating. Int J Electrochem. 2011;261:407-792. https://doi.org/10.4061/2011/261407
10. Hoppe-Hoeffler M, Germany S, Borton L et al. Electrodeposition coating composition comprising cellulose additive. United States Patent. 1995. Patent Number: 5.430078.
11. Odetola P, Popoola P, Popoola O et al. Parametric Variables in Electro-deposition of Composite Coatings: Chapter from Book, INTECH Open Science /Open Minds. 2016. http://dx.doi.org/10.5772/62010
12. Torabinejad V, Aliofkhazraei M, Assareh V et al. Electrodeposition of Ni–Fe alloys, composites, and nano coatings- A review. J Alloys Cmpd. 2017;(691) 841-859. http://dx.doi.org/10.1016/j.jallcom.2016.08.329
13. Popoola API, Aigbodion VS, Fayomi OSI. Surface characterization, mechanical properties and corrosion behaviour of ternary based Zn-ZnO-SiO_2 composite coating of mild steel. J Alloys Cmpd. 2016;654:561-566. http://doi.org/10.1016/j.jallcom.2015.09.090
14. Tamilselvi M, Kamaraj P, Arthanareeswari M et al. Nano Zinc Phosphate Coatings for Enhanced Corrosion Resistance of Mild Steel. Appl Surf Sci. 2014. http://dx.doi.org/10.1016/j.apsusc.2014.11.081
15. Rezaee N, Attar M, Ramezanzadeh B. Studying corrosion performance, microstructure and adhesion properties of a room temperature zinc phosphate conversion coating containing Mn^{2+} on mild steel. Surf Coat Technol. 2013;236: 361-367. https://doi.org/10.1016/j.surfcoat.2013.10.014

16. Lei T, Ouyang C, Tang W et al. Preparation of MgO coatings on magnesium alloys for corrosion protection. Surf Coat Technol. 2010;204:3798-3803. https://doi.org/10.1016/j.surfcoat.2010.04.060
17. Jinxia M, Zhaochuang S, Zhiguo W et al. Preparation of ZnO–cellulose nanocomposites by different cellulose solution systems with a colloid mill. Cellulose. 2016;23:3703-3715. https://doi.org/10.1007/s10570-016-1081-0
18. Meulendijks N, Burghoorn M, Mourad M et al. Electrically conductive coatings consisting of Ag-decorated cellulose nanocrystals. Cellulose. 2017;24:2191-2204. https://doi.org/10.1007/s10570-017-1240-y
19. Jinshu S, Sheldon Q, Shi H et al. Kenaf Bast Fibers—Part I: Hermetical Alkali Digestion. Int J Polym Sci. 2011. http://dx.doi.org/10.1155/2011/212047
20. Jonoobi M, Harun J, Mathew A et al. Preparation of cellulose nanofibers with hydrophobic surface characteristics. Cellulose. 2010;17:299-307. https://doi.org/10.1007/s10570-009-9387-9
21. Anyanwu BU, Adebomi OA, Fayomi OS et al. Effects of kenaf core and bast fibers as dispersing phases on low density fiberboards (engineered wood). J Phys- Conf Series. 2019;1378:022024. http://dx.doi.org/10.1088/1742-6596/1378/2/022024
22. Adebajo MO, Frost RL, Kloprogge JTK et al. Raman spectroscopic investigation of acetylation of raw cotton. Spectrochim Acta Part A: Mol Biomol Spectrosc. 2006;64(2):448-453. https://doi.org/10.1016/j.saa.2005.07.045
23. Jonoobi M, Harun J, Shakeri A et al. Chemical composition, crystallinity and thermal degradation of bleached and unbleached kenaf bast (*Hibiscus cannabinus*) pulp and nanofibers. Bioresources. 2009;4 (2):626639. https://doi.org/10.15376/BIORES.4.2.626-639
24. Chakraborty A, Sain M, Kortschot M. Cellulose Microfibrils- A novel method of preparation using high shear refining and cryo crushing. Holzforschung. 2005;59:102-10. https://doi.org/10.1515/HF.2005.016
25. Hosking NC, Strom MA, Shipway PH et al. Corrosion resistance of zinc–magnesium coated steel. Corros Sci. 2007;49:3669-3695. https://doi.org/10.1016/j.corsci.2007.03.032
26. Kadham AJ, Hassan D, Mohammad N et al. Fabrication of Polymer Blend-magnesium Oxide Nanoparticle and studying their Optical Properties for Optoelectronic Applications. Bull Elec Eng Informatics. 2018;7(1)28-34. https://doi.org/10.11591/eei.v7i1.839
27. Poedji L, Fahma R, Asri K. Modification of cellulose with acetic acid to removal of methylene blue dye. J Phys: Conf Series. 2019;1282:012079. https://doi.org/10.1088/1742-6596/1282/1/012079
28. Anyanwu BU, Oluwole OO, Fayomi OSI et al. Synthesis, corrosion and structural characterization of kenaf nanocellulose on Zn-ZnO-xCn electrolytic coatings of mild steel for advanced applications. Case Studies Chem Environ Eng. 2021;3:1-5. https://doi.org/10.1016/j.cscee.2020.100017
29. Anyanwu BU, Oluwole OO, Fayomi OSI et al. Processing and development of corrosion resistance surface-active thin film nanocellulose composite coatings for mild steel protection. Prot Metals Phys Chem Surf Springer Nat. 2021;57(6):1206-1213. https://doi.org/10.1134/S2070205121060034